COMBINING HYPERSPECTRAL UAV AND MULTISPECTRAL FORMOSAT-2 IMAGERY FOR PRECISION AGRICULTURE APPLICATIONS

C.M. Gevaert[1], J.Tang[1], F.J. García-Haro[2], J. Suomalainen[3] & L. Kooistra[3]

[1] Department of Physical Geography and Ecosystem Science, Lund University, Sölvegatan 12, S-223 62 Lund, Sweden

[2] Department of Earth Physics and Thermodynamics, University of Valencia, Dr. Moliner, 50. 46100 Burjassot, Valencia, Spain

[3] Laboratory of Geo-Information Science and Remote Sensing, Wageningen University, P.O. Box 47, 6700 AA Wageningen, The Netherlands

ABSTRACT

Remote sensing is a key tool for precision agriculture applications as it is capable of capturing spatial and temporal variations in crop status. However, satellites often have an inadequate spatial resolution for precision agriculture applications. High-resolution Unmanned Aerial Vehicles (UAV) imagery can be obtained at flexible dates, but operational costs may limit the collection frequency. The current study utilizes data fusion to create a dataset which benefits from the temporal resolution of Formosat-2 imagery and the spatial resolution of UAV imagery with the purpose of monitoring crop growth in a potato field. The correlation of the Weighted Difference Vegetation Index (WDVI) from fused imagery to measured crop indicators at field level and added value of the enhanced spatial and temporal resolution are discussed. The results of the STARFM method were restrained by the requirement of same-day base imagery. However, the unmixing-based method provided a high correlation to the field data and accurately captured the WDVI temporal variation at field level (r=0.969).

Index Terms— UAV, STARFM, unmixing-based data fusion, precision agriculture, WDVI

1. INTRODUCTION

Precision agriculture aims to maximize agricultural production in a sustainable manner by optimizing the use of input resources. This may provide economic and environmental benefits and play an important role in global food security. The key behind precision agriculture is quantifying spatial and temporal variation in crop conditions in order to apply variable management strategies within a field [1].

Remote sensing is capable of observing such variation in plant growth indicators such as canopy nitrogen content and plant biomass [2]. A number of studies describe the use of multispectral satellite imagery for precision agriculture applications [3]. However, factors such as inadequate spatial or temporal resolution and cloud cover [4] have limited the effectiveness of utilizing satellite imagery. Alternatively, Unmanned Aerial Vehicles (UAV) have been proposed for precision agriculture applications [5] as they can provide hyperspectral imagery with a higher spatial resolution and more flexible acquisition times [6]. However, operational requirements may inhibit monitoring of large areas and the frequency of flights.

Recently, much research has been done on the application of data fusion between medium-resolution imagery such as MODIS [7] and MERIS [8], [9] and high-resolution datasets such as Landsat to obtain a fused image dataset with a daily temporal resolution and a spatial resolution of 30 m. Two prevalent data fusion methods are the Spatial and Temporal Adaptive Reflectance Fusion Model (STARFM) [7] and unmixing-based data fusion [8], [9]. These methods could be adapted to fuse multispectral satellite imagery such as Formosat-2 with hyperspectral imagery obtained from an UAV platform for precision agriculture applications.

The objective of the current study is to develop a method for data fusion between Formosat-2 imagery and hyperspectral UAV imagery of a potato field in the Netherlands to obtain a fused dataset for crop monitoring in precision agriculture applications. The resulting image time series benefits from an increased temporal resolution obtained from the multispectral satellite imagery, and an increased spatial resolution obtained from the UAV dataset.

2. METHODOLOGY

2.1. Study Area

The study area is a potato field at 51°19' N and 5°10'14" E, near the village of Reusel in the Netherlands. At the beginning of the 2013 growing season, the field was divided into four zones and applied with differing initial nitrogen fertilization rates: 0, 90, 162 and 252 kgN.ha^{-1}. Six experimental plots of 13x30 m were delimited per zone, for which SPAD, LAI and spectral reflectances were measured weekly between June 6th and August 23rd, 2013. More

information regarding the experimental setup can be found in Kooistra et al. [10].

2.2. Imagery

A hyperspectral system on an UAV consisting of a Specim ImSpector V10 2/3" spectrograph mounted on an Aerialtronics Altura AT8 octocopter was developed by the Wageningen University (WU) Laboratory of Geo-information Science and Remote Sensing (GRS) under the Smart Inspectors project [10]. This UAV was flown over the study area at four dates (June 6, June 14, July 5 and July 17, 2013) to obtain imagery with 101 spectral bands at a spatial resolution of 1 m. All images have been georeferenced, orthorectified and atmospherically corrected [10].

Formosat-2 imagery have a spatial resolution of 8 m, and consists of four multispectral bands [11]. During the 2013 growing season, 42 Formosat-2 images were available over the study area. However, only eight dates were cloud-free: April 24, June 6, June 8, July 2, July 8, July 18, July 22, and August 2, 2013. The cloud-free images were georeferenced and radiometrically corrected using the coefficients provided in the metadata. The QUAC method [12] was applied to atmospherically correct the Formosat-2 image of June 6th. An empirical line correction was then applied between all the other Formosat-2 images and the June 6th image, to calibrate the spectral signature throughout the time series. Finally, calibration coefficients were obtained from the UAV and Formosat-2 images of June 6th, and all Formosat-2 images were calibrated to the UAV imagery.

2.3. Data fusion

The current study made use of two data fusion algorithms: an unmixing-based algorithm and STARFM. The unmixing-based algorithm is based on previous works by [8], [9]. It considers a linear mixing model in which the resolution of the medium-resolution imagery is assumed to be a summation of the spectra of each endmember within the pixel weighted by the abundance of the endmember within the pixel. The endmembers are obtained by performing a clustering algorithm, in this case a k-means clustering, on the high-resolution input data (i.e. the UAV imagery). The abundances of each endmember can be calculated by overlaying the medium-resolution imagery and the high-resolution unsupervised classification. The unmixing-based method is applied using a moving-window to allow for spectral heterogeneity of endmembers throughout the scene. Furthermore, the current application utilized Bayesian theory to restrain the unmixing process by including a priori endmember spectra selected from homogenous Formosat-2 pixels [13].

The STARFM method is based on the premise that both high- and medium-resolution imagery observe the same spectral reflectances, biased by a systematic error. This error is consistent over short spatial and temporal intervals. Using a reference pair of high- and medium-resolution images on a base date, the bias is calculated by selecting neighbors based on selection criteria [7] within a set search distance to form a linear system of equations. Once the bias has been obtained from the base image pair, it can then be applied to a medium-resolution image on a different day to obtain a synthetic high-resolution image. In the current application, Formosat-2 provided the medium-resolution imagery and the UAV provided the high-resolution imagery. To apply the STARFM method, both sources of imagery must have corresponding spectral bands. Therefore, the spectral bands of the hyperspectral UAV imagery corresponding to the wavelengths of each of the four Formosat-2 bands was averaged to create a UAV image with four spectral bands.

The input parameters of each algorithm were first optimized by applying data fusion to the UAV imagery on June 6th and the Formosat-2 imagery on July 17th, which allowed for the comparison of the fused image to the actual UAV image of July 17th. For the unmixing-based method, the moving window size was varied from 3x3 to 29x29 Formosat-2 pixels in steps of 4 and the number of spectral clusters was varied from 2 to 16 in steps of 2. The quality of the fusion was determined by calculating the spectral and spatial ERGAS [14]. For the STARFM method, the maximum search distance was varied from 15 m to 105 m, and the number of spectral slices was varied from 10 to 40. The fusion quality was analyzed by calculating Pearson's correlation and the RMSE to the ground-truth UAV image.

Next, data fusion was applied to each Formosat-2 image. For the unmixing-based method, each Formosat-2 image was fused with the closest preceding UAV image. As there was no UAV image preceding April 24th, this Formosat-2 image was fused with the UAV image on June 6th. The STARFM method requires an input base pair of Formosat-2 and UAV imagery on the same date. Therefore, only the UAV images on June 6th and July 17th could be used to create the data fusion time series.

2.4. Validation

The Weighted Difference Vegetation Index (WDVI) [15] was used to calculate the correlation between the imagery and the field data. The SPAD measurements were converted to leaf chlorophyll using the coefficients presented by [16], and multiplied by the LAI to obtain canopy chlorophyll measurements. The image WDVI, field WDVI, LAI and canopy chlorophyll were averaged to plot level. The imagery on the dates June 6, July 2, July 18 and August 2 were compared to the field data on June 6, July 5, July 17, and July 31, assuming that a 3-day interval presented no
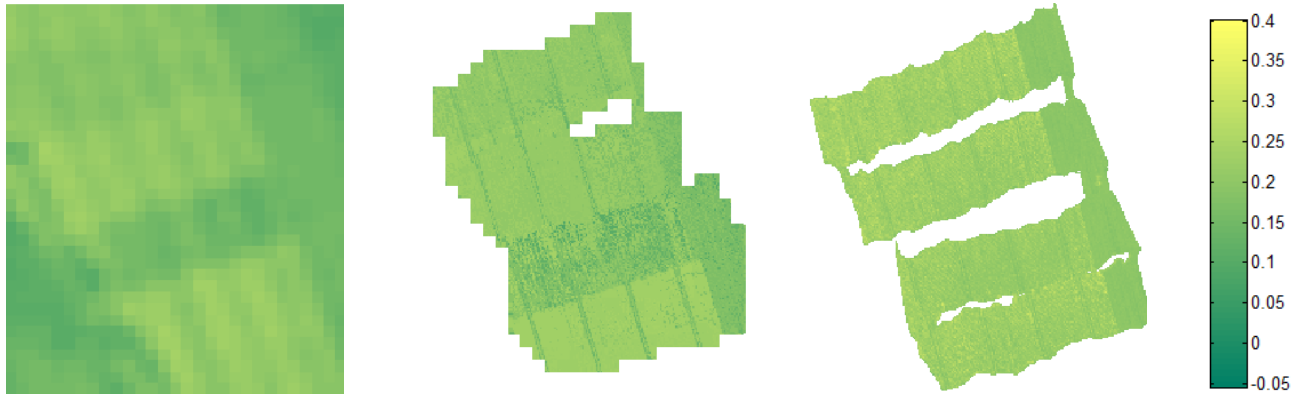
Fig. 1. WDVI on July 8th calculated from the Formosat-2 satellite image (left), the fused product of the unmixing-based algorithm (center), and obtained from through STARFM (right).

Table 1. Pearson's correlation coefficient between the average WDVI per plot calculated from imagery and reference data. All correlations are significant at p<0.001.

Reference indicator	Unmixing	STARFM	UAV	F2
Field WDVI	0.969	0.677	0.935	0.966
LAI	0.896	0.528	0.927	0.905
Canopy chlorophyll (g/m^2)	0.788	0.337	0.902	0.810

significant changes to the WDVI. Furthermore, temporal WDVI profiles were made for an experimental plot receiving no initial fertilization.

3. RESULTS AND DISCUSSION

In the parameter optimization stage for unmixing, a window size of 9x9 Formosat-2 pixels and 10 clusters obtained the best quality indicators (spatial ERGAS = 2.76; spectral ERGAS = 0.98). STARFM produced the best results with a search distance of 105 m and 30 spectral slices (r=0.715; RMSE = 0.133×10^{-5}). However, through all the variations in input parameters, the STARFM correlation coefficient only varied between 0.710 and 0.715 and the RMSE varied from 1.335 – 1.345 $\times 10^{-5}$. This suggests that STARFM is relatively insensitive to variations in the input parameters in the current application, and future applications could dedicate less time to the parameter optimization phase.

The WDVI calculated from the Formosat-2 imagery has a high correlation to crop status indicators (Table 1), which indicates that it contains relevant information regarding crop status and is a valuable input for data fusion methods. The unmixing-based method provides similar correlation coefficients to the Formosat-2 imagery. This is expected as the spectral information in the unmixing-based data is derived from the Formosat-2 imagery, and the correlation coefficients presented in Table 1 are averaged at a plot level of 15x30 m. The added spatial resolution is thus not taken into account in these correlation coefficients, although Figure 1 clearly illustrates the added value of the improved spatial resolution.

The STARFM method presented the lowest correlation to the field observations, which is likely due to the use of only two of the UAV images as high-resolution input for the fused time series. As the unmixing-based method can utilize all four UAV images as input, spatial variation is captured at an earlier stage in the growing season. For the image on July 8th, for example, unmixing-based fusion could utilize the input UAV image on July 5th and thus correctly differentiates the vegetation status of the different nitrogen application rate zones (Figure 1). As there is no corresponding Formosat-2 image on July 5th, the STARFM method must use the imagery of June 6th as a base date and cannot differentiate crop growth variation between fertilizer application-rate zones.

From each image source, temporal profiles can be constructed to analyze the crop status during the growing season. Figure 2 presents the temporal WDVI profiles of one of the experimental plots receiving no initial fertilization. The UAV WDVI closely follows the field observations, but no UAV imagery is available after July 17th. The STARFM method once again clearly shows the influence of the input base image pair, and does not provide consistent results in the current study. However, the relative temporal variation of the Formosat-2 and unmixing-based imagery follows the temporal pattern of the field data – although the WDVI is systematically lower. During the growing season, the farmer applied additional fertilization in mid-July which causes the increase in WDVI at this time. There was no UAV imagery available after this date to capture the changes, but the increase in WDVI is correctly captured in the unmixing-based WDVI profile. This is an
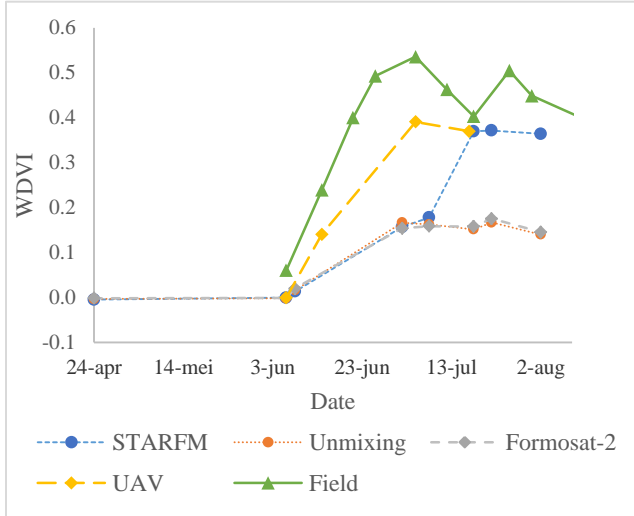
Fig. 2. Temporal WDVI profiles of an experimental plot receiving no initial fertilization.

example of the added value of the enhanced temporal resolution provided by data fusion.

4. CONCLUSIONS

The current study demonstrates the utility of applying data fusion methods to combine satellite imagery with UAV imagery for precision agriculture applications. The STARFM method is limited in the current situation by the requirement of base imagery from both sources on the same date and therefore presents temporally unstable results. This could be mitigated by coinciding UAV operations with satellite collection dates in future studies. The unmixing-based method presented a high correlation to the WDVI (r=0.969), LAI (r=0.896) and canopy chlorophyll (r=0.788) measured at field level. The WDVI obtained from unmixing-based data fusion presented a bias to the UAV WDVI, which is likely due to differing processing chains of the UAV and Formosat-2 data. However, the relative phenological variations were more accurately captured by the time series created by the unmixing-based method. This study indicates how the fused dataset can combine temporal resolution of the Formosat-2 imagery and the spatial resolution of the UAV imagery for precision agriculture applications.

4. ACKNOWLEDGEMENTS

5. REFERENCES

[1] R. Gebbers and V. I. Adamchuk, "Precision agriculture and food security.," *Science*, vol. 327, no. 5967, pp. 828–31, Feb. 2010.
[2] J. G. P. W. Clevers and L. Kooistra, "Using Hyperspectral Remote Sensing Data for Retrieving Canopy Chlorophyll and Nitrogen Content," *IEEE J. Sel. Top. Appl. Earth Obs. Remote Sens.*, vol. 5, no. 2, pp. 574–583, Apr. 2012.
[3] M. Diacono, P. Rubino, and F. Montemurro, "Precision nitrogen management of wheat. A review," *Agron. Sustain. Dev.*, vol. 33, no. 1, pp. 219–241, Sep. 2012.
[4 D. J. Mulla, "Special Issue : Sensing in Agriculture Review Twenty five years of remote sensing in precision agriculture : Key advances and remaining knowledge gaps 5," *Biosyst. Eng.*, vol. 114, no. 4, pp. 358–371, Apr. 2013.
[5] J. A. J. Berni, S. Member, P. J. Zarco-tejada, L. Suárez, and E. Fereres, "Thermal and Narrowband Multispectral Remote Sensing for Vegetation Monitoring From an Unmanned Aerial Vehicle," *IEEE Trans. Geosci. Remote Sens.*, vol. 47, no. 3, pp. 722–738, 2009.
[6] C. Zhang and J. Kovacs, "The application of small unmanned aerial systems for precision agriculture: a review," *Precis. Agric.*, vol. 13, no. 6, pp. 693–712, Jul. 2012.
[7] F. Gao, J. Masek, M. Schwaller, and F. Hall, "On the blending of the Landsat and MODIS surface reflectance: predicting daily Landsat surface reflectance," *IEEE Trans. Geosci. Remote Sens.*, vol. 44, no. 8, pp. 2207–2218, Aug. 2006.
[8] J. Amorós-López, L. Gómez-Chova, L. Alonso, L. Guanter, R. Zurita-Milla, J. Moreno, and G. Camps-Valls, "Multitemporal fusion of Landsat/TM and ENVISAT/MERIS for crop monitoring," *Int. J. Appl. Earth Obs. Geoinf.*, vol. 23, pp. 132–141, Aug. 2013.
[9] R. Zurita-Milla, J. G. P. W. Clevers, and M. E. Schaepman, "Unmixing-Based Landsat TM and MERIS FR Data Fusion," *IEEE Geosci. Remote Sens. Lett.*, vol. 5, no. 3, pp. 453–457, 2008.
[10] L. Kooistra, J. Suomalainen, S. Iqbal, J. Franke, P. Wenting, and H. Bartholomeus, "Crop monitoring using a light-weight hyperspectral mapping system for unmanned aerial vehicles : first results for the 2013 season," in *Workshop on UAV-based Remote Sensing Methods for Monitoring Vegetation*, 2013, no. September, pp. 1–7.
[11] C.-C. Liu, "Processing of FORMOSAT-2 Daily Revisit Imagery for Site Surveillance," *IEEE Trans. Geosci. Remote Sens.*, vol. 44, no. 11, pp. 3206–3214, Nov. 2006.
[12] L. S. Bernstein, S. M. Adler-Golden, R. L. Sundberg, R. Y. Levine, T. C. Perkins, A. Berk, A. J. Ratkowski, G. Felde, and M. L. Hoke, "Validation of the QUick Atmospheric Correction (QUAC) algorithm for VNIR-SWIR multi- and hyperspectral imagery," in *SPIE 5806, Algorithms and Technologies for Multispectral, Hyperspectral, and Ultraspectral Imagery XI*, 2005, vol. 5806, pp. 668–678.
[13] C. M. Gevaert and F. J. García-Haro, "A Comparison of STARFM and an Unmixing-based Algorithm for Landsat and MODIS Data Fusion," Manuscript submitted for publication, 2014.
[14] L. Wald, *Data Fusion: Definitions and Architectures : Fusion of Images of Different Spatial Resolutions*. Paris, France: Presses des MINES, 2002, p. 198.
[15] J. G. P. W. Clevers, "Application of a weighted infrared-red vegetation index for estimating leaf Area Index by Correcting for Soil Moisture," *Remote Sens. Environ.*, vol. 29, no. 1, pp. 25–37, Jul. 1989.
[16] J. Uddling, J. Gelang-Alfredsson, K. Piikki, and H. Pleijel, "Evaluating the relationship between leaf chlorophyll concentration and SPAD-502 chlorophyll meter readings.," *Photosynth. Res.*, vol. 91, no. 1, pp. 37–46, Jan. 2007.